Chapter 2

R-matrix Theory

The reaction(R-) matrix theory was developed by Brueckner and others to discuss nuclear matter and liquid ^{3}He in 3D [1]. They calculated the effective interaction in 3D liquid ^{3}He using this theory and found that the interaction in the d-wave channel was the most attractive. Now it is known that their conclusions were incorrect [2]. The major reason for the failure is that the R-matrix theory cannot take proper account of the effect of spin fluctuations, which are strongly enhanced in 3D liquid ^{3}He and generate the effective attractive interaction responsible for the occurrence of the p-wave superfluidity. The R-matrix theory takes account of only the two-particle correlation.

In contrast to 3D ^{3}He, one can change the areal density ρ_{2D} of 2D ^{3}He considerably; for example, the areal density ρ_{2D} of submonolayer 2D ^{3}He on graphite can be changed by a factor of about 5, $0.01\text{Å}^{-2} \lesssim \rho_{2D} \lesssim 0.06\text{Å}^{-2}$ [3, 4, 5, 6, 7, 8]. In 3D, the density can be hardly changed and the uniform susceptibility, which is a good measure of the correlation effect of the system, is always strongly enhanced. In the dilute 2D ^{3}He, the enhancement of the uniform susceptibility is modest [4]. It is thus clear that the R-matrix theory is valid for 2D ^{3}He at least in the dilute limit.

We apply the R-matrix theory to 2D liquid ^{3}He to calculate the effective interaction and the possible transition temperatures. In Subsection 2.1.2, we introduce the R-matrix approximation, where the effect of the surrounding particle is considered only through the fermi distribution function, i.e., through the restriction of the phase space available for two scattering particles (holes). Neglect of the fermi distribution function reduces the R-matrix approximation to the simple scattering problem. We calculate the effective interaction between ^{3}He atoms and estimate the superfluid transition temperature. In Subsection 2.1.3, we study the effect of the surrounding atoms by introducing the selfenergy which is made of the particle-particle (hole-hole) T-matrix. In principle, the T-matrix has to be calculated self-consistently,

and the R-matrix has to be calculated using the dispersion of quasiparticles, which is readily obtained once the selfenergy is calculated; the R-matrix obtained in this way is called the K-matrix [1]. We call the method using the K-matrix the K-matrix approximation. We also calculate the effective interaction using the the K-matrix approximation.

2.1   Formulation

2.1.1   Model Hamiltonian

We begin with the second-quantized Hamiltonian

$$
\mathcal{H}^{(A)} = \sum_{k,\sigma} \xi_k a^{\dagger}_{k\sigma} a_{k\sigma}
$$
$$
+ \frac{1}{2} \sum_q V(|q|) \sum_{k,k',\sigma,\sigma'} a^{\dagger}_{k+q\sigma} a^{\dagger}_{k'-q\sigma'} a_{k'\sigma'} a_{k\sigma},
\tag{2.1}
$$

where $a_{k\sigma}(a^{\dagger}_{k\sigma})$ is the annihilation(creation) operator of a ^{3}He atom of momentum $k = (k_x, k_y)$ and spin σ, ξ_k is the kinetic energy measured from the chemical potential μ, $\xi_k = \frac{k^2}{2m_3} - \mu$ and $V(|q|)$ is Fourier transformation of the interaction potential $V(r)$ between ^{3}He atoms. Here m_3 is the atomic mass of ^{3}He.

The interaction between ^{3}He atoms is a combination of a hard core repulsion at a short distance and the weak van der Waals attraction at medium and long distances. The Lennard-Jones potential [9, 10] is used as the interaction potential between ^{3}He atoms,

$$
V(r) = 4\varepsilon \left[(\frac{\sigma}{r})^{12} - (\frac{\sigma}{r})^6 \right].
\tag{2.2}
$$

The parameters σ and ε are $\sigma = 2.56\text{Å}$ and $\varepsilon = 10.2$ K respectively.

A technical problem with the Lennard-Jones potential is the strong divergence for small r (a hard core). To avoid it, we use a modified potential, which is free from the divergence at $r \to 0$,

$$
V(r) = \left\{ \begin{array}{ll} Ar^2 + B & 0 \leq r \leq r_c \\ 4\varepsilon \left[(\frac{\sigma}{r})^{12} - (\frac{\sigma}{r})^6 \right] & r \geq r_c \end{array} \right. ,
\tag{2.3}
$$

where A and B are chosen so that $V(r)$ and its derivative become continuous at $r = r_c$. In Fig. 2.1, we show the modified potential for $r_c = 0.9\sigma$.
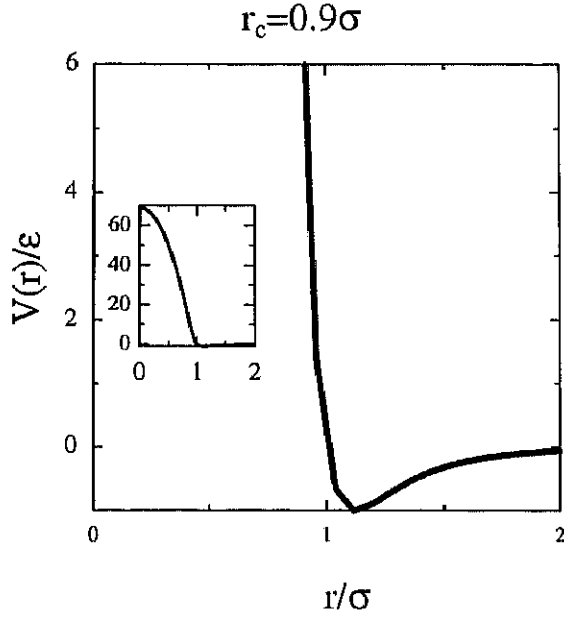
14

Figure 2.1: The modified Lennard-Jones potential for $r_c = 0.9\sigma$, which is free from the divergence at $r \to 0$.

We must confirm that results are independent of r_c. We find that as r_c decreases the results such as the effective interaction converge to constant values; the convergence is almost complete for $r_c \lesssim 0.8\sigma$. In Fig. 2.2, we show the dependence of the effective interaction λ_m on r_c for $\rho_{2D} = 0.020\text{Å}^{-2}$ and $\varepsilon_c = 0.2\varepsilon_F$ (See the next subsection about the definitions of λ_m and ε_c). As seen in Fig. 2.2, the convergence is almost complete for $r_c \lesssim 0.8\sigma$. In the following, we present results obtained for $r_c = 0.3\sigma$.
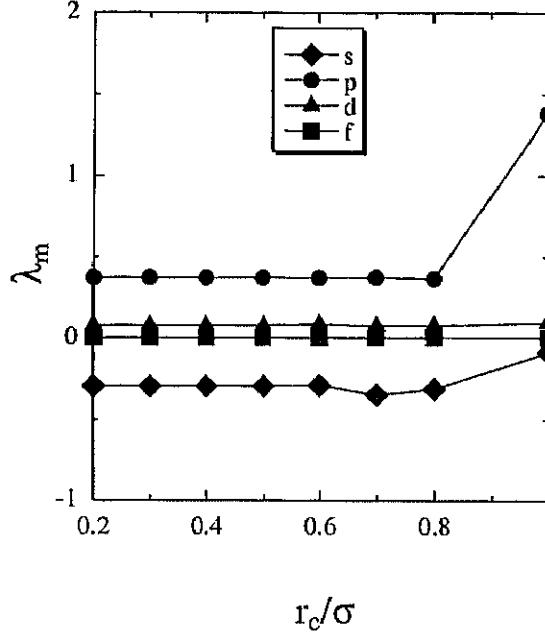
15

Figure 2.2: Dependence of the effective interaction λ_m on r_c for $\rho_{2D} = 0.020\text{Å}^{-2}$ and $\varepsilon_c = 0.2\varepsilon_F$

2.1.2 R-matrix approximation

We introduce a vertex function $\mathcal{T}(K; k, k')$ satisfying the integral equation

$$\mathcal{T}(K; k, k') = V(|k - k'|) - \sum_{k''} V(k - k'')G^{(0)}(k'')G^{(0)}(K - k'')\mathcal{T}(K; k'', k'), \quad (2.4)$$

Where we use the following abbreviations: $k = (k, i\varepsilon_n)$ and $\Sigma_k = \frac{1}{S}\Sigma_k\Sigma_n$ where $\varepsilon_n = (2n+1)\pi T$ with T being temperature and n being integer and S is the system volume, Which is assumed to be unity in the following. Equation (2.4) is diagrammatically given in Figs. 2.3. $G^{(0)}(k)$ is the Green's function of a non-interacting fermion,

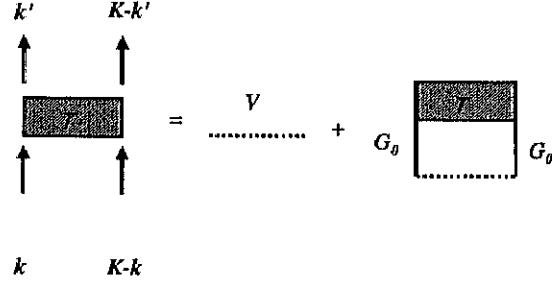$$G^{(0)}(k) = \frac{1}{i\varepsilon_n - \xi_k}. \quad (2.5)$$

16

Figure 2.3: Diagrammatic expression for the integral equation to be satisfied by a vertex function $\mathcal{T}(K; k, k')$. The dashed line represents the interaction and the solid line represents the Green's function $G^{(0)}$ of a non-interacting fermion. On the left-hand side, external lines are included for clarity.

In Eqs. (2.4) and (2.5), spin indices are neglected. Note that a vertex function $\mathcal{T}(K; k, k')$ is not antisymmetrized.

As $V(|q|)$ is independent of frequency, it can easily be seen that $\mathcal{T}(K; k, k')$ depends neither on ε_n nor on $\varepsilon_{n'}$, and Eq. (2.4) is written as

$$\mathcal{T}(K; k, k') = V(|k - k'|) - \sum_{k''} V(|k - k''|) L(K; k'') \mathcal{T}(K; k'', k') \qquad (2.6)$$

where

$$L(K; k) = \sum_{n} G^{(0)}(k) G^{(0)}(K - k) = -\frac{1 - f(\xi_k) - f(\xi_{K-k})}{i\Omega_m - \xi_k - \xi_{K-k}}, \qquad (2.7)$$

$f(\xi)$ is fermi distribution function and $\Omega_m = 2m\pi T$ with m being integer.

As we are interested in the effective interaction between ^{3}He atoms of momentum k_F and $-k_F$ (k_F is the fermi momentum), we calculate $\bar{\mathcal{T}}(k, k') = \mathcal{T}(0; k, k')$, which satisfies the integral equation,

$$\bar{\mathcal{T}}(k, k') = V(|k - k'|) - \sum_{k''} V(|k - k''|) \frac{(1 - 2f(\xi_{k''}))}{2\xi_{k''}} \bar{\mathcal{T}}(k'', k'). \qquad (2.8)$$

It is noted that, in the absence of the exclusion principle, Eq. (2.8) is reduced to

17

the two-body scattering equation. At $T = 0$, Eq. (2.8) is written by

$$\bar{\mathcal{T}}(k, k') = V(|k - k'|) - \sum_{k''} \frac{V(|k - k''|)}{2|\xi_{k''}|} \bar{\mathcal{T}}(k'', k'). \tag{2.9}$$

As the potential $V(r)$ is short-ranged, it is more convenient to transform to the coordinate space. We introduce the wave matrix $\Omega(K)$ by

$$\mathcal{T}(K; k, k') = \sum_{k''} V(|k - k''|) < k''|\Omega(K)|k' > . \tag{2.10}$$

We define the wave function $\Psi_k(K; r)$ by

$$\Psi_k(K; r) = < r|\Omega(K)|k > . \tag{2.11}$$

Then, Eq. (2.9) can be written in terms of Ψ_k as

$$\Psi_k(r) = e^{ik \cdot r} - \int d^2r L(|r - r'|) V(r') \Psi_k(r'), \tag{2.12}$$

where

$$L(r) = \sum_k \frac{e^{ik \cdot r}}{2|\xi_k|} = \frac{1}{(2\pi)} \int_0^\infty dk \frac{k J_0(kr)}{2|\xi_k|}, \tag{2.13}$$

$J_0(z)$ is the Bessel function and $\Psi_k(0; r)$ is abbreviated by $\Psi_k(r)$. Using Eqs. (2.10) and (2.11), we can show

$$\bar{\mathcal{T}}(k, k') = \int d^2r e^{-ik \cdot r} V(r) \Psi_{k'}(r). \tag{2.14}$$

Once $\bar{\mathcal{T}}(k, k')$ is obtained, it is easy to calculate the effective interaction λ_m ($m = 0, 1, 2, \cdots$), where m stands for the magnitude of the angular momentum:

$$\lambda_m = \frac{1}{2\pi} \int_0^{2\pi} \cos(m\theta_{k_F, k_F'}) \bar{\mathcal{T}}(k_F, k_F') d\theta_{k_F, k_F'}, \tag{2.15}$$

where $\theta_{k, k'}$ is the angle between k and k'.

Thus far we have not yet discussed the singularity on the second term of the right-hand side of Eq. (2.9) or Eq. (2.13). Now we have to specify how to avoid the singularity. We understand the integral on the right-hand side of Eq. (2.9) and Eq. (2.13) as principal integrals; thus $\mathcal{T}(K; k, k')$ is understood to be the R-matrix. In fact, taking the principal part is not sufficient to obtain useful results for the

effective interaction. To see this, suppose, for the momentum, $V(k)$ to be constant V_0. Equation (2.9) is then easily solved and the solution is

$$\bar{\mathcal{T}}(k, k') = \bar{\mathcal{T}} = \frac{V_0}{1 + V_0 \sum_k L(k)} \qquad (2.16)$$

which simply vanishes at $T = 0$ because $\sum_k L(k)$ logarithmically diverges. From this it is difficult to obtain useful information on the effective interaction and the transition temperature caused by it. We then introduce a cut off ε_c in Eq. (2.9) or Eq. (2.13); for example, Eq. (2.13) is changed to

$$L(r) \to L(r; \varepsilon_c) = \sum_{|\xi_k| > \varepsilon_c} \frac{e^{ik \cdot r}}{2|\xi_k|} = \frac{1}{(2\pi)} \int_0^\infty dk \frac{k J_0(kr)}{2|\xi_k|} \theta_1\left(\frac{|\xi_k|}{\varepsilon_c}\right), \qquad (2.17)$$

where

$$\theta_1(x) = \left\{ \begin{array}{ll} 1 & |x| > 1 \\ 0 & |x| < 1 \end{array} \right. , \qquad (2.18)$$

Then $\bar{\mathcal{T}}(k, k')$ and consequently the effective interaction λ_m depends on the cut off ε_c. We can show, however, that the superfluid transition temperature hardly depends on the cut off ε_c. To show this, we again assume $V(k)$ to be constant and negative, $V(k) = V_0 < 0$.(constant $V(k)$ induces only the Cooper pairing of s-wave symmetry. Extension to deal with non-s-wave channels is straightforward.) Equation (2.16) is then written as

$$\bar{\mathcal{T}}(k, k') \simeq \frac{|V_0|}{1 - N_0 |V_0| \ln \frac{\varepsilon_F}{\varepsilon_c}}, \qquad (2.19)$$

where N_0 is the density of states at the fermi surface,

$$N_0 = \sum_k \delta(\xi_k) = \frac{m_3}{2\pi \hbar^2}. \qquad (2.20)$$

Introducing ε_0 by

$$1 = N_0 |V_0| \ln \frac{\varepsilon_F}{\varepsilon_0}, \qquad (2.21)$$

we can rewrite Eq. (2.19) as

$$\bar{\mathcal{T}}(k, k') \simeq \frac{1}{N_0 \ln \frac{\varepsilon_c}{\varepsilon_0}}, \qquad (2.22)$$

(We assume that $\varepsilon_0 < \varepsilon_c$.). From this, we can see that the effective interaction λ_m logarithmically depends on ε_c,

$$N_0 \lambda_m \simeq \frac{1}{\ln \frac{\varepsilon_c}{\varepsilon_0}}. \tag{2.23}$$

On the other hand, having integrated out the high-energy process, $|\xi_k| > \varepsilon_c$, we can regard λ_m as the effective interaction between atoms near the fermi surface, $|\xi_k| < \varepsilon_c$. We therefore obtain the expression for the transition temperature $T_c^{(m)}$ as

$$T_c^{(m)} = 1.13\varepsilon_c \exp(-\frac{1}{N_0|\lambda_m|}). \tag{2.24}$$

Substituting Eq. (2.23) into Eq. (2.24), we finally obtain

$$T_c^{(m)} \simeq \varepsilon_0, \tag{2.25}$$

which does not depend on ε_c. We have indeed confirmed the insensitivity of the transition temperature $T_c^{(m)}$ on ε_c (See Figs. 2.4). In the following, we fix the value of ε_c to be $0.2\varepsilon_F$: $\varepsilon_c = 0.2\varepsilon_F$

In Appendix 2.A, we show that the estimation of the transition temperature T_c using the method described above can be justified as far as $T_c \ll \varepsilon_F$.

2.1.3 K-matrix approximation

We also use the K-matrix approximation to calculate the effective interaction. We introduce a vertex function $T(K, k, k')$, satisfying the integral equation

$$T(K, k, k') = V(|k - k'|) - \sum_{k''} V(|k - k''|)G(k'')G(K - k'')T(K; k'', k'), \tag{2.26}$$

which is diagrammatically shown in Fig. 2.5. The dressed Green's function $G(k)$ is given by

$$G(k) = \frac{1}{i\varepsilon_n - \xi_k - \Sigma(k)}, \tag{2.27}$$

where the self-energy $\Sigma(k)$ is given by (See Fig. 2.6),

$$\Sigma(k) = 2 \sum_{k'} T(k + k'; k, k)G(k') - \sum_{k'} T(k + k'; k, k')G(k'). \tag{2.28}$$

The factor of 2 of the first term arises from the summation of spin. Spin indices are neglected in Eqs. (2.26), (2.27) and (2.28). It should be noted that when the
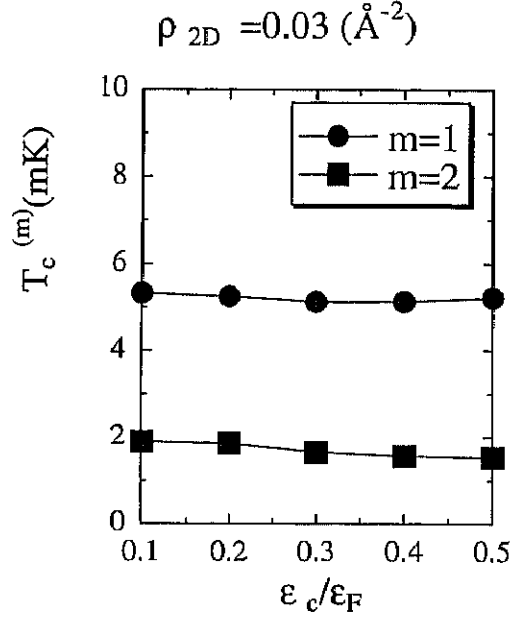
20

$\rho_{2D} = 0.03$ (Å^{-2})

$T_c^{(m)}$ (mK)

10

8

● — m=1
■ — m=2

6

4

2

0

0.1   0.2   0.3   0.4   0.5

$\varepsilon_c/\varepsilon_F$

Figure 2.4: Dependence of the transition temperatures, $T_c^{(1)}$ (solid circles) and $T_c^{(2)}$ (solid squares), on the energy cut off ε_c

dressed Green's function $G(k)$ is replaced by the Green's function $G^{(0)}(k)$ of a non-interacting fermion, $T(K; k, k')$ is reduced to $\mathcal{T}(K; k, k')$.

Since $T(K; k, k')$ also depends neither on ε_n nor on $\varepsilon_{n'}$, Eq. (2.26) is rewritten as

$$T(K; k, k') = V(|k - k'|) - \sum_{k''} V(|k - k''|) M(K; k'') T(K; k'', k'), \qquad (2.29)$$

where

$$M(K; k) = T \sum_{n'} G(k') G(K - k'). \qquad (2.30)$$
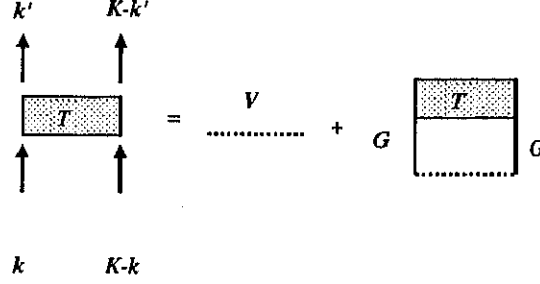
21

k' K-k'

T = V + G T G

k K-k

Figure 2.5: Diagrammatic expression for the integral equation to be satisfied by a vertex function $T(K, k, k')$. The dashed line represents the interaction and the solid line represents the dressed Green's function G. On the left-hand side, external lines are included for clarity.

Similarly, Eq. (2.28) is rewritten as

$$\Sigma(k) = 2 \sum_{k'} T(k + k'; k, k) G(k') - \sum_{k'} T(k + k'; k, k') G(k'). \qquad (2.31)$$

Equations (2.29) , (2.30) and (2.31) constitute self-consistent equations. However, it is difficult to solve self-consistent equations (2.29) , (2.30) and (2.31) in a continuous model because of the enormous computation time [1] . In this study we neglect the frequency dependence of the K-matrix for simplicity, i.e. $T(K; k, k') \rightarrow T(\boldsymbol{K}; \boldsymbol{k}, \boldsymbol{k'})$. Since the summation of the frequency, $\sum_{i\varepsilon_n}$, of the selfenergy can then be performed analytically (See Eq. (2.36)), the numerical effort is suppressed dramatically and we can solve self-consistent equations with a moderate numerical effort.

We can easily show that the selfenergy also becomes independent of the frequency, i.e. $\Sigma(k) \rightarrow \Sigma(\boldsymbol{k})$ and Eq. (2.31) is written as

$$\Sigma(k) = \Sigma(\boldsymbol{k}) = 2 \sum_{\boldsymbol{k'}} T(\boldsymbol{k} + \boldsymbol{k}; \boldsymbol{k}, \boldsymbol{k}) \sum_{n'} G(k') - \sum_{\boldsymbol{k'}} T(\boldsymbol{k} + \boldsymbol{k'}; \boldsymbol{k}, \boldsymbol{k'}) \sum_{n'} G(k'). \qquad (2.32)$$

---

[1] In lattice models the self-consistent equations can be solved since the FFT algorithm can be applied (See the next chapter).
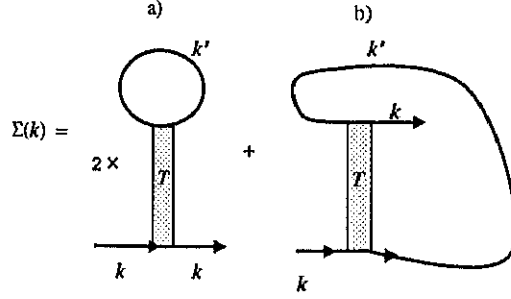
Figure 2.6: Diagrams representing selfenergy $\Sigma(k)$; (a) the direct term and (b) the exchange term. The solid line represents the dressed Green's function G. External lines are also included for clarity.

Since the selfenergy $\Sigma(k)$ is independent of the frequency $i\varepsilon_n$, the Green's function $G(k)$ is written as

$$G(k) = \frac{1}{i\varepsilon_n - E_k} \tag{2.33}$$

where the quasiparticle dispersion E_k is defined as

$$E_k = \xi_k + \Sigma(k). \tag{2.34}$$

It is then easy to show

$$T\sum_{n'} G(k') = f(E_{k'}), \tag{2.35}$$

and that

$$\Sigma(k) = 2\sum_{k'} T(k + k'; k, k)f(E_{k'}) - \sum_{k'} T(k + k'; k, k')f(E_{k'}), \tag{2.36}$$

and

$$M(K; k) = -\frac{1 - f(E_k) - f(E_{K-k})}{i\Omega_m - E_k - E_{K-k}}. \tag{2.37}$$

Substituting Eq. (2.37) into Eq. (2.29), we have

$$T(K; k, k') = V(|k - k'|) - \sum_{k''} V(|k - k''|)T(K; k'', k')\frac{1 - f(E_{k''}) - f(E_{K-k''})}{E_{k''} + E_{K-k''} - Z}, \tag{2.38}$$

23

where we replace $i\Omega_m$ by a real number Z.

Although we have assumed that $T(K; k, k')$ is independent of frequency, we still have frequency Z on the right-hand side of Eq. (2.38), i.e., the approximation is not self-consistent. To make the approximation self-consistent, we have to get rid of the Z-dependence of Eq. (2.38) appropriately. It is reasonable to replace Z by the total energy of the "incident" particles, $Z = E_k + E_{K-k}$ in Eq. (2.38). This is indeed close to the approximation used by Brueckner et al. [1].

It is again more convenient to transform to the coordinate space. We introduce the wave matrix $\tilde{\Omega}(K)$ by

$$T(K; k, k') = \sum_{k''} V(|k - k''|) < k'' - \frac{K}{2} |\tilde{\Omega}(K)| k' - \frac{K}{2} > . \qquad (2.39)$$

We define the wave function $\tilde{\Psi}_k(K; r)$ by

$$\tilde{\Psi}_k(K; r) = < r |\tilde{\Omega}(K)| k - \frac{K}{2} > . \qquad (2.40)$$

Then we can obtain

$$T(K; k, k') = \int d^2 r\, e^{-i(k - \frac{K}{2}) \cdot r} V(r) \tilde{\Psi}_{k'}(K; r). \qquad (2.41)$$

Equation (2.38) can be written in terms of $\tilde{\Psi}_k(K; r)$ as

$$\tilde{\Psi}_k(K; r) = e^{i(k - \frac{K}{2}) \cdot r} - \int d^2 r'\, M(K, Z; r - r') V(r') \tilde{\Psi}_k(K; r') \qquad (2.42)$$

where

$$M(K, Z; r) = -\sum_{k''} \frac{1 - f(E_{\frac{K}{2} - k''}) - f(E_{\frac{K}{2} + k''})}{Z - E_{\frac{K}{2} - k''} - E_{\frac{K}{2} + k''}} e^{ik'' \cdot r}, \qquad (2.43)$$

and

$$Z = E_{K-k} + E_k. \qquad (2.44)$$

Note that $k - \frac{K}{2}$ is the relative momentum of the scattering particles.

Since there is a singularity on the second term on the right-hand side of Eq. (2.38) (or Eq. (2.43)), we have to specify how to avoid the singularity. The method we use here is to replace

$$\frac{1}{x} \rightarrow \frac{x}{x^2 + \delta^2}, \qquad (2.45)$$

24

where x is the energy denominator in Eq. (2.38) (or Eq. (2.43)) and δ is a small positive value.

In fact, it is still difficult to obtain a self-consistent solution for Eqs. (2.36), (2.41), (2.42) and (2.43). We then make the following approximation closely following Brueckner *et al.* [1]: (1) we replace $t_0(K;k'') \equiv 1 - f(E_{\frac{K}{2}-k''}) - f(E_{\frac{K}{2}+k''})$ with its angular average in Eq. (2.43);

$$t_0(K;k'') \to t_0(K;k'') \equiv <<t_0(K;k'')>> = \frac{1}{2\pi}\int_0^{2\pi} d\theta_{K,k''} t_0(K;k''). \quad (2.46)$$

We easily obtain $t_0(K;k'')$,

$$t_0(K;k'') = \begin{cases} -1 \ , \ k'' + \dfrac{K}{2} \le k_F \\[2mm] -1 + \dfrac{2}{\pi}\arctan\dfrac{\sqrt{1-|c|^2}}{|c|} \ , \ \sqrt{k''^2 + \dfrac{K^2}{4}} \le k_F \le k'' + \dfrac{K}{2} \\[2mm] 1 - \dfrac{2}{\pi}\arctan\dfrac{\sqrt{1-|c|^2}}{|c|} \ , \ |k'' - \dfrac{K}{2}| \le k_F \le \sqrt{k''^2 + \dfrac{K^2}{4}} \\[2mm] 1 \ , \ k_F \le k'' - \dfrac{K}{2}, \end{cases} \quad (2.47)$$

where

$$c = \frac{1}{k''K}[k_F^2 - (k''^2 + \frac{K^2}{4})]. \quad (2.48)$$

(2) Furthermore, we consider the polynomial expansion of E_k, $E_k = E_0 + Ak^2 + Bk^4 + \cdots$. Then $<<E_{\frac{K}{2}+k''} + E_{\frac{K}{2}-k''}>>$ is written by

$$<<E_{\frac{K}{2}+k''} + E_{\frac{K}{2}-k''}>> \quad (2.49)$$

$$\simeq \ 2[E_0 + A(k''^2 + \frac{K^2}{4}) + B(k''^2 + \frac{K^2}{4})^2] + 2B<<(k\cdot K)^2>> \quad (2.50)$$

$$= \ 2[E_0 + A(k''^2 + \frac{K^2}{4}) + B(k''^2 + \frac{K^2}{4})^2 + \frac{1}{2}k''^2 K^2] \simeq E_{K_+} + E_{K_-}, \quad (2.51)$$

where

$$K_\pm \equiv \sqrt{k''^2 + \frac{K^2}{4} \pm \sqrt{\frac{k''^2 K^2}{2}}} \quad (2.52)$$

Resorting to approximations (1) and (2), we have

$$M(k+k',Z;r) \to M(|k+k'|,Z;r) = -\frac{1}{2\pi}\int_0^\infty dk'' \frac{k''t_0(|k+k'|;k'')J_0(k''r)}{Z - E_{K_+} - E_{K_-}}, \quad (2.53)$$

25

that is, $M(k + k', Z; r)$ depends only on magnitude of $|k + k'|$ and of r. We finally have the self-consistent equations to be solved;

$$E_{\underline{k}} = \xi_{\underline{k}} + 2 \sum_{|\underline{k}'| < k_F} T(k + k'; k, k) - \sum_{|\underline{k}'| < k_F} T(k + k'; k, k'), \qquad (2.54)$$

$$\tilde{\Psi}_{\underline{k}}(|k + k'|; r) = e^{i(\frac{\underline{k} - \underline{k}'}{2}) \cdot r} - \int d^2 r' M(|k + k'|, Z; |r - r'|) V(r') \tilde{\Psi}_{\underline{k}}(|k + k'|; r'), \qquad (2.55)$$

$$M(|k + k'|, Z; r) = -\frac{1}{2\pi} \int_0^{\infty} dk'' k'' t_0(|k + k'|; k'') \frac{(Z - E_{K_+} - E_{K_-})}{(Z - E_{K_+} - E_{K_-})^2 + \delta^2}, \qquad (2.56)$$

$$Z = E_{\underline{k}} + E_{\underline{k}'}, \qquad (2.57)$$

and

$$T(k + k'; k, k') = \int d^2 r e^{-i(\frac{\underline{k} - \underline{k}'}{2}) \cdot r} V(r) \tilde{\Psi}_{\underline{k}'}(|k + k'|; r), \qquad (2.58)$$

where we use the relation, $\Psi_{\underline{k}}(k + k'; r) = \Psi_{\underline{k}}(|k + k'|; r)$. Once $E_{\underline{k}}$ is obtained by solving self-consistent equations (2.54), (2.55), (2.56) and (2.58), we easily obtain the effective interaction $\tilde{\lambda}_m$,

$$\tilde{\lambda}_m = \frac{1}{2\pi} \int_0^{2\pi} d\theta \cos(m\theta) \bar{T}(k_F, k_F'), \qquad (2.59)$$

where $\bar{T}(k, k')$ is given by

$$\bar{T}(k, k') = V(|k - k'|) - \sum_{|E_{\underline{k}''}| > \varepsilon_c} \frac{V(|k - k''|)}{2|E_{\underline{k}''}|} \bar{T}(k'', k'). \qquad (2.60)$$

The superfluid transition temperature $\tilde{T}_c^{(m)}$ is given by

$$\tilde{T}_c^{(m)} = 1.13 \varepsilon_c \exp(-\frac{1}{\tilde{N}_0 |\tilde{\lambda}_m|}), \qquad (2.61)$$

where $\tilde{N}_0$ is the density of states at the fermi surface,

$$\tilde{N}_0 = \sum_{\underline{k}} \delta(E_{\underline{k}}) = \frac{k_F}{2\pi} \frac{1}{(\frac{dE_{\underline{k}}}{dk})_{k=k_F}}. \qquad (2.62)$$

26

2.2 Results

2.2.1 R-matrix approximation

In this subsection, the results obtained with the R-matrix approximation are shown. We calculate the effective interaction and the superfluid transition temperatures for $0.005\text{Å}^{-2}\lesssim\rho_{2D}\lesssim0.055\text{Å}^{-2}$, which is the experimentally accessible areal density of 2D ^{3}He.

We solve Eq. (2.12) for $\Psi_{\vec{k}}(r)$ for $0 < r < R$ with $R = 3\sigma$. The integration on the right-hand side of Eq. (2.12) is discretized: $R = N_r\Delta_r$ and $2\pi = N_\phi\Delta_\phi$. We show results obtained for $N_r = 80$ and $N_\phi = 30$.

In Fig. 2.7, the effective interactions λ_m are shown as functions of the areal density; the cut-off ε_c is fixed at $\varepsilon_c = 0.2\varepsilon_F$. When the areal density ρ_{2D} is low,
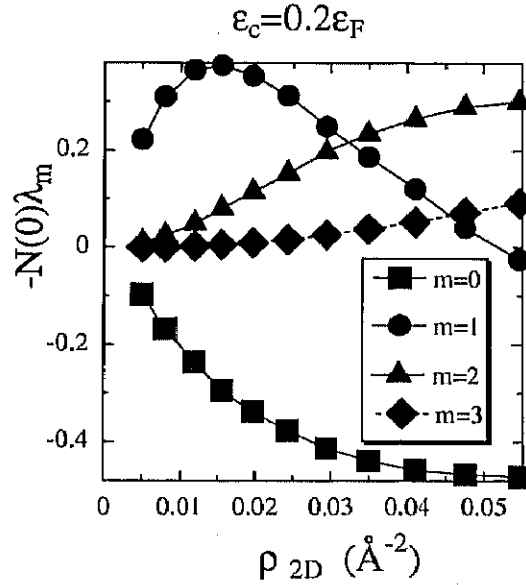

Figure 2.7: The effective interactions λ_m as functions of areal density ρ_{2D}.

27

$\rho_{2D} \lesssim 0.033 \text{Å}^{-2}$, the effective interaction λ_1 in the p-wave channel is the most attractive. When the areal density ρ_{2D} is high, $\rho_{2D} \gtrsim 0.033 \text{Å}^{-2}$, the effective interaction λ_2 in the d-wave channel is the most attractive. For $0.005 \text{Å}^{-2} \lesssim \rho_{2D} \lesssim 0.055 \text{Å}^{-2}$, we find no attractive interaction in the s-wave channel. We find, however, in the dilute limit, $\rho_{2D} \lesssim 0.003 \text{Å}^{-2}$, the effective interaction in the s-wave channel becomes attractive.

Next we estimate the superfluid transition temperature by Eq. (2.24). In Fig. 2.8, the superfluid transition temperatures $T_c^{(1)}$ and $T_c^{(2)}$ are shown as functions of the areal density. The transition temperature to the p-wave superfluidity is 1-10 mK for the low density region, $\rho_{2D} \lesssim 0.033 \text{Å}^{-2}$.
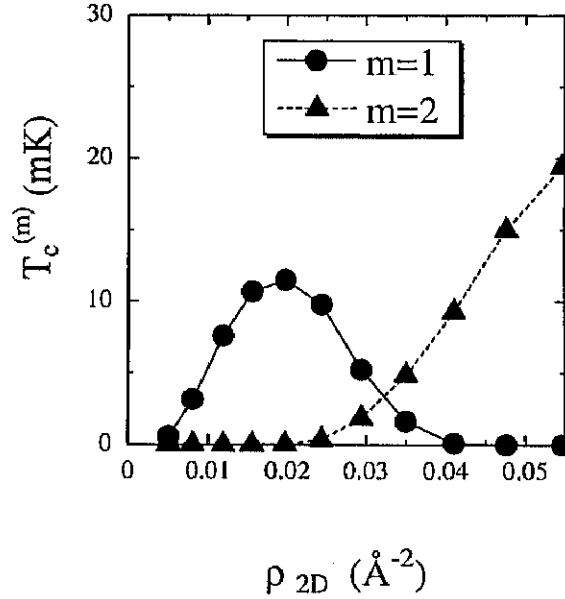

Figure 2.8: The p-wave superfluid transition temperature $T_c^{(1)}$ (solid circles) and the d-wave superfluid transition temperature $T_c^{(2)}$ (solid triangles) as functions of areal density ρ_{2D}.

2.2.2 K-matrix approximation

In this subsection, the results obtained with the K-matrix approximation are shown. The problem is to find a self-consistent solution of Eqs. (2.54), (2.55), (2.56) and (2.58). We obtain self-consistent solutions by iterations starting from the energy dispersion of non-interacting particles, $E_k = \xi_k = \frac{k^2}{2m} - \mu$. One iteration consists of calculating the output energy dispersion $E_k^{(\text{out})}$ from the input energy dispersion $E_k^{(\text{in})}$. Firstly, using $E_k^{(\text{in})}$, we calculate Eq. (2.56). The integration on the right-hand side of Eq. (2.56) is discretized: [2]

$$0 \leq k'' \leq \frac{16}{\sigma}, \Delta k'' = \frac{\frac{16}{\sigma}}{60}. \tag{2.64}$$

We then solve Eq. (2.55) to obtain $\tilde{\Psi}_k(K; r)$. The integration on the right-hand side of Eq. (2.55) is discretized:

$$0 \leq r' \leq 3\sigma, \Delta r' = \frac{3\sigma}{15} \text{ and } 0 \leq \theta' \leq 2\pi, \Delta \theta' = \frac{2\pi}{15}. \tag{2.65}$$

The mesh used for the calculation of Eq. (2.54) is

$$0 \leq k' \leq k_F, \Delta k' = \frac{k_F}{10} \text{ and } 0 \leq \theta' \leq 2\pi, \Delta \theta' = \frac{2\pi}{10}. \tag{2.66}$$

We calculate Eq. (2.54) to obtain $E_k^{(\text{out})}$ at the discretized values;

$$0 \leq k \leq k_0, \Delta k = \frac{k_0}{10}, \tag{2.67}$$

where we choose k_0 to be $2k_F$. In Eq. (2.56), we need more E_k's than calculated using Eq. (2.54). For those E_k's, we use a spline interpolation and we put

$$E_k = \xi_k = \frac{k^2}{2m} - \mu \text{ for } k > k_0. \tag{2.68}$$

The condition for the convergence is

$$|E_k^{(\text{in})} - E_k^{(\text{out})}| < 0.1\varepsilon_F \sim 0.001\varepsilon_F \text{ for } 0 \leq k \leq k_0. \tag{2.69}$$

---

[2] We use the following abbreviation about a mesh:

$$k_1 \leq k \leq k_2, \Delta k = \frac{(k_2 - k_1)}{N}, \tag{2.63}$$

where k stands for a variable, k_1 and k_2 stands for the upper limit and the lower limit respectively, and the mesh of k consists of N values.

In Fig. 2.9, we show the obtained quasiparticle dispersion E_k for several values of the areal density. The results are shifted so that $E_{k=k_F} = 0$. For comparison the dispersion ξ_k of a non-interacting particles is also shown. As the density increases, the slope of E_k becomes small for $k \lesssim k_F$, i.e., the quasiparticle effective mass m_3^* increases in agreement with the experiment results [3]. The effective mass m_3^* is calculated by

$$m_3^* = \frac{\hbar^2 k_F}{(\frac{dE_k}{dk})_{k=k_F}}, \tag{2.70}$$

and is shown in Fig. 2.10 as a function of the areal density.

The transition temperatures $\tilde{T}_c^{(m)}$ calculated with dispersion E_k are shown in Fig. 2.11 together with $T_c^{(m)}$ obtained with the R-matrix approximation. For $\rho_{2D} \lesssim 0.030 \text{Å}^{-2}$, the p-wave transition temperature is the highest. The transition temperatures $\tilde{T}_c^{(m)}$ are enhanced compared with $T_c^{(m)}$ obtained with the R-matrix theory because of the enhancement of the effective mass, i.e., the density of states $\tilde{N}_0$ at the fermi surface. For $\rho_{2D} \lesssim 0.020 \text{Å}^{-2}$, however, $\tilde{T}_c^{(m)} \simeq T_c^{(m)}$, implying that the selfenergy effect is insignificant in this region. This means that the present theories — the R-matrix approximation and the K-matrix approximation — are quantitatively reliable in this region. On the other hand, for $\rho_{2D} \gtrsim 0.020 \text{Å}^{-2}$, $\tilde{T}_c^{(m)}$ deviates from $T_c^{(m)}$. In this region, the selfenergy effect is important.

2.3   Summary and discussion

We have applied the R-matrix theory to two-dimensional ^{3}He on a flat substrate to calculate possible transition temperature to a superfluid state. The R-matrix approximation gives the transition temperatures of the order of mK. For $\rho_{2D} \lesssim 0.033 \text{Å}^{-2}$, the p-wave transition temperature is the highest. For $\rho_{2D} \gtrsim 0.033 \text{Å}^{-2}$, the d-wave transition temperature is the highest. In the K-matrix approximation, which takes account of the selfenergy effect, the p-wave transition temperature is the highest and remains of the order of mK for $\rho_{2D} \lesssim 0.020 \text{Å}^{-2}$. We find that the selfenergy effect is irrelevant for the low density region, $\rho_{2D} \lesssim 0.020 \text{Å}^{-2}$. This implies that the present theory is valid for $\rho_{2D} \lesssim 0.020 \text{Å}^{-2}$.

We neglect dynamical effects such as the damping effect of the selfenergy and the retardation effect of the effective interaction in the present theory. These effects will reduce the transition temperature to some degree. However, these effects are expected to be small in the dilute region.

Since the system is two-dimensional, the transition will be a Kosterlitz-Thouless (KT) transition [11]. The KT transition temperature T_{KT} is generally smaller than
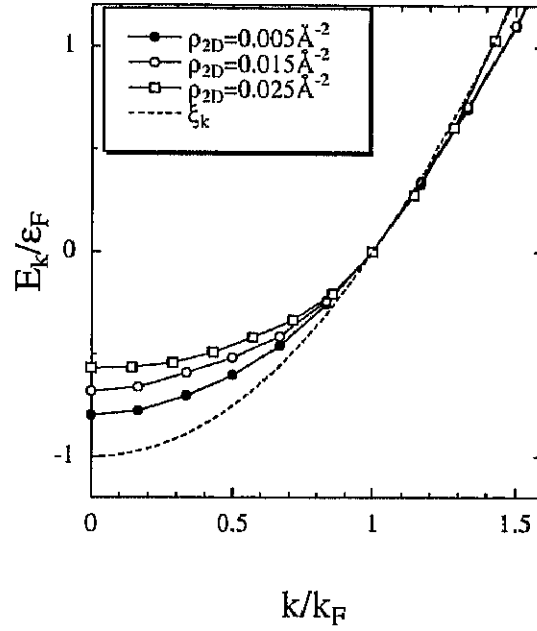
30

$\rho_{2D}=0.005\overset{\circ}{A}^{-2}$

$\rho_{2D}=0.015\overset{\circ}{A}^{-2}$

$\rho_{2D}=0.025\overset{\circ}{A}^{-2}$

ξ_k

E_k/ε_F

k/k_F

Figure 2.9: The quasiparticle dispersions E_k obtained with the K-matrix approximation for several values of the areal densityρ_{2D}: $\rho_{2D} = 0.005\overset{\circ}{A}^{-2}$, $\rho_{2D} = 0.015\overset{\circ}{A}^{-2}$ and $\rho_{2D} = 0.025\overset{\circ}{A}^{-2}$. The results are normalized by the fermi energy $\varepsilon_F = \frac{k_F^2}{2m_3}$. The dashed line stands for the free dispersion $\xi_k = \frac{k^2}{2m_3} - \varepsilon_F$.
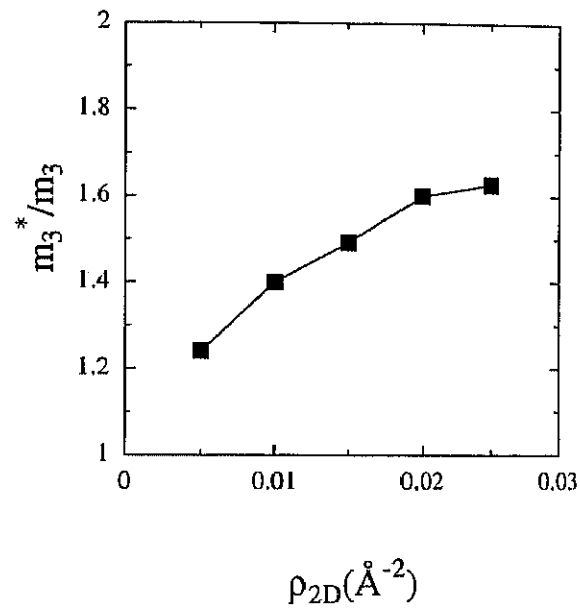
Figure 2.10: The quasiparticle effective mass m_3^* as a function of the areal density ρ_{2D}.
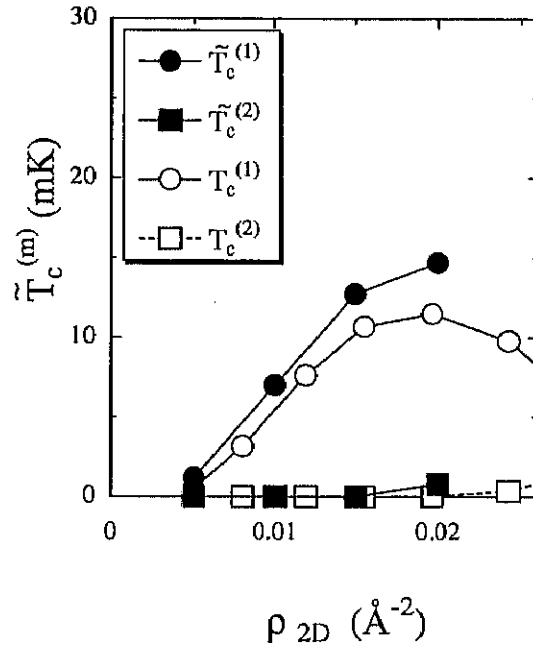
Figure 2.11: The superfluid transition temperatures $\tilde{T}_c^{(1)}$ and $\tilde{T}_c^{(2)}$ obtained with the K-matrix approximation.

the "mean field" transition temperature T_c, which we have calculated. From the theory of the KT transition, there is a jump of the areal superfluid density $\rho_s(T_{KT})$ at the transition temperature T_{KT}. The areal superfluid density $\rho_s(T_{TK})$ at the transition temperature is given by $\frac{\rho_s(T_{TK})}{\rho_{2D}} = 2\frac{T_{KT}}{T_F}$, where $T_F = \frac{\hbar^2 \pi \rho_{2D}}{m_3 k_B}$. We crudely estimate the difference of the two transition temperatures by $\frac{T_c - T_{KT}}{T_{KT}} \sim \frac{\rho_s(T_{KT})}{\rho_{2D}} = 2\frac{T_{KT}}{T_F}$. From this, we can see that the difference of the two transition temperatures is negligibly small when $\frac{T_{KT}}{T_F} \ll 1$ [12]. Therefore, the actual transition temperature is reliably estimated by the "mean field" transition temperature T_c if T_c is of the order of mK [3] .

Our conclusion is for pure two-dimensional systems. In fact, the actual system is not free from the randomness of the substrate. It reduces the onset of non-s-wave superfluidity and can localize ^{3}He atoms. To realize superfluidity, it is essential to suppress the randomness. Another problem is a system size of 2D plane. If the transition temperature is of the order of 1 mK, the coherence length of the superfluid state is of the order of 100 Å. The area of 2D plane has to be at least greater than 100 nm^2 in order for superfluidity to be free from the size effect, which is considered to suppress the transition temperature. For example, however, the Grafoil surface consists of many platelets, whose typical size is 40-100 nm^2 [5, 6], which is at most the size of a Cooper pair. This can be one of the reasons why superfluidity has not been observed yet although the temperature is lowered down to 100μK [6].

Chubukov and Sokol [13] discussed the properties of liquid ^{3}He adsorbed on graphite on the basis of Landau fermi liquid theory. They found that the dominant attractive interaction was in the p-wave channel and estimated the p-wave transition temperature to be of the order of mK for moderate areal density. The present results are consistent with theirs, and provide a microscopic basis of their theory at least in the dilute region.

The present theory can not be reliably applied to the high density region, $\rho_{2D} \gtrsim 0.020$Å^{-2}, where correlation effect is important, and cannot predict anything on a superfluid transition in that region. We believe that a paramagnon theory, which was successfully applied to 3D ^{3}He [14, 15, 16, 17, 18], will also be useful in the high density region, because spin fluctuations are also strongly enhanced there in 2D. We study what type of pairing the strong spin fluctuations leads to in 2D in the next chapter.

---

[3] T_F is of the order of 1 K for the areal density region of 2D ^{3}He.

Appendix

2.A The effective interaction and the estimation of the transition temperature T_c

Here we reformulate the integral equation for the vertex function $\bar{T}(k, k')$, Eq. (2.8), and show that the method of the estimation of the transition temperature T_c in §2.1 can be justified as far as $T_c \ll \varepsilon_F$.

The integral equation for $\bar{T}(k, k')$ reads

$$\bar{T}(k, k') = V(|k - k'|) - \sum_{k''} V(|k - k''|) L(k'') \bar{T}(k'', k'), \tag{2.71}$$

where

$$L(k) = \frac{1 - 2f(\xi_k)}{2\xi_k}, \tag{2.72}$$

at a finite temperature. The transition temperature T_c is determined as the temperature where $\bar{T}(k_F, k'_F)$ diverges (Thouless's criterion). If the transition temperature were similar in magnitude to ε_F, it would be easy to solve Eq. (2.71) directly to obtain the transition temperature. However, in the present case, the transition temperature turns out to be much smaller than ε_F. In this case, one has to solve Eq. (2.71) accurately at exponentially small temperatures to obtain the transition temperature, which is a difficult numerical task. However, we can take advantage of the fact that $T_c \ll \varepsilon_F$ and solve Eq. (2.71) accurately in two steps [19].

Equation (2.71) can also be expressed as a series expansion,

$$
\begin{aligned}
\bar{T}(k, k') &= V(|k - k'|) - \sum_{k_1} V(|k - k_1|) L(k_1) V(|k_1 - k'|) \\
&+ \sum_{k_1} \sum_{k_2} V(|k - k_1|) L(k_1) V(|k_1 - k_2|) L(k_2) V(|k_2 - k'|) \\
&+ \cdots .
\end{aligned}
\tag{2.73}
$$

In the series expansion, each summation of wave number can be divided into the summation near the fermi surface and the summation far away from the fermi surface,

$$\sum_k = \sum_L + \sum_H, \tag{2.74}$$

35

where

$$\sum_L = \sum_{|\xi_k|<\varepsilon_c} ,$$ (2.75)

and

$$\sum_H = \sum_{|\xi_k|>\varepsilon_c} ,$$ (2.76)

where an energy cut off ε_c is introduced. The choice of ε_c will be discussed later.

We define $W(k, k')$ as the series where only the summations far way from the fermi surface are included,

$$
\begin{aligned}
W(k, k') &= V(|k - k'|) - \sum_{H_1} V(|k - k_1|)L(k_1)V(|k_1 - k'|) \\
&\quad + \sum_{H_1}\sum_{H_2} V(|k - k_1|)L(k_1)V(|k_1 - k_2|)L(k_2)V(|k_2 - k'|) \\
&\quad + \cdots .
\end{aligned}
$$ (2.77)

Note that $W(k, k')$ depends on the energy cut off ε_c. One can readily see that $W(k, k')$ satisfies an integral equation,

$$W(k, k') = V(|k - k'|) - \sum_{H''} V(|k - k''|)L(k'')W(k'', k'). $$ (2.78)

In §2.1, we used the same notation $\mathcal{T}(k, k')$ even when the cut off ε_c was introduced. Here, we introduce another notation $W(k, k')$ to avoid confusion. Note that then, strictly speaking, $\mathcal{T}(k, k')$ in Eq. (2.14) and Eq. (2.15) should be written as $W(k, k')$.

Now we rearrange Eq. (2.71) or Eq. (2.73) in terms of $W(k, k')$. First we collect all the terms where only one summation near the fermi surface is involved;

$$
-\sum_{L_1} V(|k - k_1|)L(k_1)V(|k_1 - k'|)
$$

$$
+(\sum_{L_1}\sum_{H_2} + \sum_{H_1}\sum_{L_2})V(|k - k_1|)L(k_1)V(|k_1 - k_2|)L(k_2)V(|k_2 - k'|)
$$

$$
-(\sum_{L_1}\sum_{H_2}\sum_{H_3} + \sum_{H_1}\sum_{L_2}\sum_{H_3} + \sum_{H_1}\sum_{H_2}\sum_{L_3})V(|k - k_1|)L(k_1)V(|k_1 - k_2|)L(k_2)
$$
$$
V(|k_2 - k_3|)L(k_3)V(|k_3 - k'|) + \cdots .
$$ (2.79)

Denoting the wave number restricted to the vicinity of the fermi surface by p, we can see that those terms are cast into the following expression,

$$-\sum_L W(k, p)L(p)W(p, k'). $$ (2.80)

36

In Eq. (2.73), there are $(n-1)$ summations of the wave numbers $(k_1, k_2, \cdots, k_{n-1})$ in the nth term on the right-hand side. Those terms where two of the $(n-1)$ summations of the wave numbers are restricted to the vicinity of the fermi surface are similarly cast into the expression,

$$\sum_{L_1} \sum_{L_2} W(k, p_1) L(p_1) W(p_1, p_2) L(p_2) W(p_2, k'), \qquad (2.81)$$

where p_1 and p_2 are restricted to the vicinity of the fermi surface. Extending these arguments, we finally find that $\bar{\mathcal{T}}(k, k')$ can be expressed in terms of $W(k, k')$ as

$$\begin{aligned}
\bar{\mathcal{T}}(k, k') &= W(k, k') - \sum_{L_1} W(k, p_1) L(p_1) W(p_1, k') \\
&+ \sum_{L_1} \sum_{L_2} W(k, p_1) L(p_1) W(p_1, p_2) L(p_2) W(p_2, k') + \cdots, \qquad (2.82)
\end{aligned}$$

that is, $\bar{\mathcal{T}}(k, k')$ satisfies the integral equation

$$\bar{\mathcal{T}}(k, k') = W(k, k') - \sum_L W(k, p) L(p) \bar{\mathcal{T}}(p, k'). \qquad (2.83)$$

In particular, the transition temperature can be determined by solving the integral equation,

$$\bar{\mathcal{T}}(k_F, k'_F) = W(k_F, k'_F) - \sum_L W(k_F, p) L(p) \bar{\mathcal{T}}(p, k'_F). \qquad (2.84)$$

What we have shown thus far is just a formal rearrangement; instead of solving Eq. (2.71) directly, we can solve it in two steps using Eq. (2.78) and Eq. (2.83). Now we show that we can *easily* calculate the transition temperature by using Eq. (2.78) and Eq. (2.83) and by taking advantage of the fact $T_c \ll \varepsilon_F$.

We can choose the cut off ε_c satisfying the condition $T_c \ll \varepsilon_c \ll \varepsilon_F$ when $T_c \ll \varepsilon_F$. Consequently, we can make two simplifications. The one is that we can solve Eq. (2.78) at $T = 0$. Strictly speaking, we also have to solve Eq. (2.78) at finite temperatures $(T \gtrsim T_c)$, which would be a difficult task as mentioned before. Temperature enters Eq. (2.78) through the fermi distribution function $f(\xi_k)$ in $L(k)$. As the wave vector k is restricted so that $|\xi_k| > \varepsilon_c$, we can safely put $T = 0$ in $L(k)$ and the resultant error is of the order of $\exp(-\varepsilon_c/T_c)$ $(\ll 1)$.

The other simplification is that we can put the magnitude of the arguments p in $W(k_F, p)$ and in $\bar{\mathcal{T}}(p, k'_F)$ in the second term on the right-hand side of Eq. (2.84) to be equal to k_F, because $\varepsilon_c \ll \varepsilon_F$;

$$\bar{\mathcal{T}}(k_F, k'_F) = W(k_F, k'_F) - \sum_L W(k_F, p_F) L(p) \bar{\mathcal{T}}(p_F, k'_F). \qquad (2.85)$$

Then, $W(k_F, k'_F)$ and $\bar{\mathcal{T}}(k_F, k'_F)$ are functions of the angle θ between k_F and k'_F only, and can be expanded as

$$W(k_F, k'_F) = \sum_{m=0}^{\infty} s_m W_m \cos(m\theta), \qquad (2.86)$$

where $s_0 = 1$ and $s_m = 2(m \geq 1)$ ($\bar{\mathcal{T}}(k_F, k'_F)$ can also be expanded similarly). Coefficients W_m is expressed as

$$W_m = \frac{1}{2\pi} \int_0^{2\pi} \cos(m\theta) W(k_F, k'_F) d\theta, \qquad (2.87)$$

and we can see that $W_m = \lambda_m$ (See Eq. (2.15). Note that in §2.1, we did not distinguish $\bar{\mathcal{T}}(k, k')$ and $W(k, k')$. In Eq. (2.15), we should use $W(k, k')$ as mentioned before). It is then straightforward to solve Eq. (2.85), and the result is

$$\bar{\mathcal{T}}_m = \frac{W_m}{1 - N_0 W_m L_c}, \qquad (2.88)$$

where

$$L_c = \int_0^{\varepsilon_c} \frac{1}{\xi} \tanh(\frac{\beta \xi}{2}) d\xi, \qquad (2.89)$$

from which the transition temperature $T_c^{(m)}$ is calculated as

$$T_c^{(m)} = 1.13 \varepsilon_c \exp(-\frac{1}{N_0 |W_m|}). \qquad (2.90)$$

This is identical to Eq. (2.24) because $W_m = \lambda_m$.

References

[1] K. A. Brueckner, T. Soda, P. W. Anderson, and P. Morel: Phys. Rev. **118** (1960) 1442.

[2] A. J. Leggett: Rev. Mod. Phys. **47** (1975) 331.

[3] D. S. Greywall: Phys. Rev. B. **41** (1990) 1842.

[4] C. P. Lusher, B. P. Cowan and J. Saunders: Phys. Rev. Lett. **67** (1991) 2497.

[5] D. S. Greywall and P. A. Busch: Phys. Rev. Lett **65** (1990) 64.

[6] M. Morishita, K. Ishida, Y. Yawata, H. Nagatani and H. Fukuyama: J. Low. Temp. Phys. **110** (1998) 351.

[7] C. Bäuerle, Yu. M. Bunkov, A. S. Chen, S. N. Fisher and H. Godfrin: J. Low. Temp. Phys **110** (1998) 333.

[8] A. Casey, H. Patel, J. Nyéki, B. P. Cowan and J. Saunders: J. Low. Temp. Phys **113** (1998) 293.

[9] J. De Boer and A. Michels: Physica **5** (1938) 945.

[10] J. De Boer and L. J. Lunbeck: Physica **14** (1948) 510.

[11] J. M. Kosterlitz and D. J. Thouless: J. Phys. **C6** (1973) 1181.

[12] K. Miyake: Prog. Theor. Phys. **69** (1983) 1749.

[13] A.V. Chubukov and A. Sokol: Phys. Rev. **49** (1994) 678.

[14] S. Nakajima: Prog. Theor. Phys. **50** (1973) 1101.

[15] P. W. Anderson and W. F. Brinkman: Phys. Rev. Lett. **30** (1973) 1108.

[16] W. F. Brinkman and P. W. Anderson: Phys. Rev. A **8** (1973) 2732.

[17] W. F. Brinkman, J. W. Serene and P. W. Anderson: Phys. Rev. A **10** (1974) 2786.

[18] Y. Kuroda: Prog. Theor. Phys. **51** (1974) 1269.

[19] P. W. Anderson and P. Morel: Phys. Rev. **123** (1961) 1910.